Hindawi
Mathematical Problems in Engineering
Volume 2022, Article ID 1622243, 15 pages
https://doi.org/10.1155/2022/1622243

Research Article

Predicting Extreme Dynamic Response of Offshore Jacket Platform Subject to Harsh Environment

Saeed Khalaj,[1] **Farshad BahooToroody**,[1] **Leonardo Leoni**,[2] **Filippo De Carlo**,[2] **Gianpaolo Di Bona**,[3] **and Antonio Forcina**[4]

[1]*Department of Civil Engineering, University of Parsian, Qazvin, Iran*
[2]*Department of Industrial Engineering (DIEF), University of Florence, Florence, Italy*
[3]*Department of Civil and Mechanical Engineering, University of Cassino and Southern Lazio, Cassino, Italy*
[4]*Department of Engineering, University Parthenope, Department of Engineering Centro Direzionale, Naples, Italy*

Correspondence should be addressed to Filippo De Carlo; filippo.decarlo@unifi.it

Received 12 April 2021; Revised 26 January 2022; Accepted 4 February 2022; Published 24 February 2022

Academic Editor: Salvatore Caddemi

Offshore jacket platforms (OJPs) may be exposed to harsh environmental conditions during their operation in different return periods. It is necessary to evaluate the dynamic performance of the OJPs subjected to extreme wave loadings to secure a safe operation. In the earlier studies, various approaches were introduced to analyze the response of an OJP in different sea states. However, the serious shortcoming of the proposed methods is computationally time consuming and requires a considerable amount of simulations to evaluate the performance of the OJP. Accordingly, these approaches would not analyze the dynamic performance of the OJP realistically. In this study, the dynamic performance of an OJP subject to a harsh environment is evaluated considering a time-domain simulation. The developed model will result in a more realistic response by simulating the whole structure subjected to 1800 seconds of extreme wave loading in the light of the sea environment randomness. The application of the methodology is demonstrated by assessing the performance of a fabricated OJP subjected to extreme wave loadings in the North Sea. The dynamic analysis shows that among all assigned probability distribution functions (PDFs), the most suitable distribution for predicting the maximum deck displacement in all return periods was generalized extreme value (GEV). Moreover, the results show that the response of the structure is likely to remain in the safe limit condition in the 1-year return period. In contrast, in other return periods, the OJP will exceed the safe limit condition. The proposed method is beneficial for future risk and reliability analyses that require a great deal of data derived from numerical simulations.

1. Introduction

The first offshore drilling platform was constructed in the Gulf of Mexico, while since the late 1940s, offshore technology has experienced extremely significant growth [1]. Although developing renewable energy resources have attracted much attention in recent years, fossil fuels, such as oil, are playing a dominant role in global energy systems. Consequently, a significant number of offshore jacket platforms (OJPs) have been fabricated and installed worldwide for drilling and preparing water or gas for injection into the reservoir for processing oil and gas [2]. Offshore structures should continue their serviceability under severe environmental conditions during the operational life span. Offshore structures are expected to carry two different loads, including gravity and environmental loads [3]. The installed structures' deadweight and corresponding elements are categorized as the gravity loads. Wave loads, as an environmental load, play a vital role in offshore structures' performance in different ocean state conditions [4]. Therefore, it is necessary to evaluate the structural behavior under extreme wave loads to examine its resistance during storm conditions. As a result, the structure's response would prove whether the demanding requirements and serviceability are accepted. The importance of evaluating the structural behavior will increase by

changing platform application and modification to the platform condition [5]. However, the existing complicated structural geometries, fluid-structure interaction (FSI), and soil-pile-structure interaction make offshore structures' assessment procedure more challenging [6]. Some guidelines and standards, such as API RP 2A [7] and ISO 19902 [8], have been proposed to assess the dynamic behaviour of the existing platforms. According to API RP 2A suggestions, a couple of analysis scenarios, including design level and ultimate strength level, should be implemented while the existing offshore structure does not meet the requirements. To carry out a linear structural analysis, employing the design level scenario is recommended, while the ultimate strength level scenario is established for nonlinear structural analysis. The ultimate strength level criteria for platforms could be satisfied by the ultimate capacity ratio to the 100-year return period wave loading. Furthermore, similar to the API RP 2A suggestions, in ISO 19902, 5 analysis levels and 2 empirical methods have been recommended. According to the structural reliability analysis basis, the level of the proposed criteria through different standards would experience a change. Reliability analysis has been carried out widely in different engineering fields to improve the systems' serviceability [9–13]. In contrast with the remarkable improvement and significant development of structural reliability theory in the last few decades, it has not been applied frequently for assessing offshore structures' performance. Researchers have proposed some procedures and approaches regarding the considerable advances in the scientific knowledge of evaluating offshore platforms' performance. Bea et al. [14, 15] proposed a straightforward procedure to evaluate fixed offshore platforms' failure probability in extreme storm conditions based on a simplified analytical formulation. Offshore platforms are assumed to be integrated systems with similar components and elements in the proposed procedure. The elements are a series of the superstructure (deck), the substructure (jacket), and the foundation (piles). Simplified formulations were employed to estimate the ultimate lateral shear capacity of the jackets. Since any platform components reach the ultimate lateral shear, the whole system will likely experience the ultimate shear capacity. The capacity of the platform elements is assessed as a function of stochastic variables. Manuel et al. [16] established a probabilistic approach to evaluate platforms' performance under extreme wave loading. A nonlinear static pushover analysis has been carried out to estimate the existing jacket platform's failure probability while the wave loading was described probabilistically. Considering the ratio of ultimate capacity in 100-year return period wave loading and annual failure rate for the fabricated platforms in the North Sea, Ersdal [17] presented a probabilistic approach. The maximum wave height that follows the Gumbel distribution plays the technical parameter in this study. The probability of failure was estimated by employing the Monte Carlo approach on the obtained simulated samples in the failure interval. The authors have neglected some possible hazards, including corrosion and pile-related failure mode since it would result in an inaccurate result. In the last decade, the performance of fixed steel jacket platforms in Katrina and Rita has been evaluated [18]. The study attempts to estimate the aforementioned installed platforms' failure probability considering seasonal storms in the Gulf of Mexico. Kjeøy et al. [19], Morandi et al. [20], and Van raaij and Gudmestad [21] have carried out studies to focus on assessing offshore structures under extreme wave loading. Beyond analyzing the platforms under different extreme wave conditions, time-history-based methods result from substantial computer processing power [6]. Regarding ocean random waves' fundamental characteristics, the time-domain method is the most reliable approach to evaluating flexible structures [19]. This method aims at evaluating the dynamic behavior of platform members subjected to the stochastic ocean wave forces as the function of time. The main shortcoming of this methodology is the time-consuming procedure in evaluating the dynamic performance of the structure.

This paper aims at predicting the extreme dynamic performance of an OJP subject to a harsh environment. At first, a time-domain stochastic wave loading was subjected to the offshore platform. The maximum deck displacements and the maximum base shear (MBS) loads were estimated for four principal return periods. Different probability distribution functions (PDFs) were then fitted on the displacements obtained from a simulation procedure to examine whether the adopted distributions would accurately predict future displacement. Finally, the structure's failure rate was projected while the structure's displacement exceeded the safe limit condition. Subsequently, to demonstrate the advantages of the proposed methodology, a real case study in the North Sea is presented.

The remaining parts of this paper are structured as follows. The subdivision of methodology is touched upon in section 2. Section 3 is devoted to applying the proposed methodology, while the concluding remarks of the paper are presented in Section 4.

1.1. Description of Software. The ultimate strength for framed offshore structures (USFOSs), a numerical commercial computer program, is utilized to analyze nonlinear static and dynamic offshore structures. The primary nonlinearity is associated with the hydrodynamic parts regarding the drag forces and stiffness of the offshore structures. The USFOS is capable of simulating the failure process in offshore space structures. The failure process takes place by evaluating the element's initial formation to the structure's final toppling [22]. The USFOS operates through green strain formulation. Although the green strain formulation is valid for large displacements, it is limited by the moderate strains as defined in the following equation:

$$\epsilon_x = u_x + \frac{1}{2}u_x^2 + \frac{1}{2}v_x^2 + \frac{1}{2}w_x^2. \quad (1)$$

By applying the Von Karman approximation [23] on the elements with low deflection, the ϵ_x would reduce to the following equation:

$$\epsilon_x = u_x + \frac{1}{2}v_x^2 + \frac{1}{2}w_x^2. \tag{2}$$

Considering the fundamental of potential energy and the virtual work principle, the stiffness of the structures' elements could be estimated. For instance, the internal strain energy of an elastic beam is estimated through the following equation:

$$U = \frac{1}{2}\int_0^1 EA\left(u_x + \frac{1}{2}v_x^2 + \frac{1}{2}w_x^2\right)^2 \mathrm{d}x + \frac{1}{2}\int_0^1 \left(EI_z v_{xx}^2 + EI_y w_{xx}^2\right)\mathrm{d}x. \tag{3}$$

The above equation consists of two integrals, while the first and second integrals represent axial straining and bending, respectively. The summation of the components in the first parenthesis shows the structural elements' strain, ϵ_x. The total displacement of the elements is assessed considering axial displacement $u(x)$, lateral deflection $v(x)$, and in three-dimension evaluation $w(x)$.

The first and second variations of the strain energy and external work potential will obtain the total and incremental equilibrium equations, respectively. The outcome of the first variation of internal strain energy, calculated using (3), is provided in the following equation:

$$\begin{aligned}\delta U = {} & \int_0^1 EAu_{,x}\delta_{u,x}\mathrm{d}x + \int_0^1 EI_z\left(v_{,xx}\delta_{v,xx} - \frac{N}{EI_z}v_{,x}\,\delta_{v,x}\right)\mathrm{d}x \\ & + \int_0^1 EI_y\left(w_{,xx}\delta_{w,xx} - \frac{N}{EI_y}w_{,x}\,\delta_{w,x}\right)\mathrm{d}x - \int_0^1 \left(N + EA_{u,x}\right)\delta_{u,x}\mathrm{d}x.\end{aligned} \tag{4}$$

The above equation, fundamental in calculating the ratio of internal equilibrium forces compared with external loads, is organized efficiently in 3 terms and 4 integrals, respectively. The first term that consists of the first integral indicates the linear contribution from the axial strain. The second term is made up of 2 integrals that show bending deformations calculated through the Livesley stability functions in the stiffness matrix. The last term comprises the last integral, describes the nonlinear axial strain contribution from lateral deflections, and clarifies the equilibrium axial loads. In mathematics, usually, the small changes in values are shown using Δ. Accordingly, (5) defines the variation of increment in strain energy.

$$\begin{aligned}\delta\Delta U = {} & \int_0^1 EA\Delta u_{,x}\delta u_{,x}\mathrm{d}x + \int_0^1 EI_z\left(\Delta v_{,xx}\delta v_{,xx}\frac{N}{EI_z}\Delta v_{,x}\delta v_{,x}\right)\mathrm{d}x \\ & + \int_0^1 EI_y\left(\Delta w_{,xx}\delta w_{,xx}\frac{N}{EI_y}\Delta w_{,x}\delta w_{,x}\right) + \int_0^1 EA\left(\Delta u_{,x}v_{,x}\delta v_{,x} + \Delta v_{,x}v_{,x}\delta u_{,x}\right)\mathrm{d}x \\ & + \int_0^1 EA\left(\Delta u_{,x}w_{,x}\delta w_{,x} + \Delta w_{,x}w_{,x}\delta u_{,x}\right) + \int_0^1 EA\Delta v_{,x}v_{,x}^2\delta v_{,x}\mathrm{d}x \\ & + \int_0^1 EA\Delta w_{,x}w_{,x}^2\delta w_{,x}\mathrm{d}x \\ & + \int_0^1 EA\left(\Delta v_{,x}v_{,x}w_{,x}\delta w_{,x} + \Delta w_{,x}w_{,x}v_{,x}\delta v_{,x}\right)Ex \\ & + \text{higher order terms.}\end{aligned} \tag{5}$$

To give a comprehensive analysis of elements' displacement, the incremental stiffness is presented through the interpolation functions.

$$\begin{aligned} u(x) &= \varnothing^T q_u, \\ v(x) &= \varnothing^T q_v, \\ w(x) &= \varnothing^T q_w. \end{aligned} \tag{6}$$

Regarding the above equation, the variation of increment in strain energy in (5) could be rewritten as follows:

$$\begin{aligned} \delta\Delta U = {} & \delta u^T \int_0^1 EA\varnothing_{u,x}\varnothing_{u,x}^T \mathrm{d}x\, \Delta u + \delta v^T \int_0^1 EI_z \left(\varnothing_{v,xx}\varnothing_{v,xx}^T \left(\frac{N}{EI_z}\right)\varnothing_{v,x}\varnothing_{v,x}^T \right)\mathrm{d}x\Delta v \\ & + \delta w^T \int_0^1 EI_z \left(\varnothing_{w,xx}\varnothing_{w,xx}^T \frac{N}{EI_z}\varnothing_{w,x}\varnothing_{w,x}^T \right)\mathrm{d}x\Delta w \\ & + \delta v^T \int_0^1 EA\, \varnothing_{v,x}\, v_{,x}\, \varnothing_{u,x}^T\, \mathrm{d}x\Delta u \\ & + \delta u^T \int_0^1 EA\, \varnothing_{u,x}\, v_{,x}\, \varnothing_{v,x}^T\, \mathrm{d}x\Delta v \\ & + \delta w^T \int_0^1 EA\, \varnothing_{w,x}\, w_{,x}\, \varnothing_{u,x}^T\, \mathrm{d}x\Delta u \\ & + \delta u^T \int_0^1 EA\, \varnothing_{u,x}\, w_{,x}\, \varnothing_{w,x}^T\, \mathrm{d}x\Delta w \\ & + \delta v^T \int_0^1 EA\, \varnothing_{v,x}\, v^2{}_{,x}\, \varnothing_{v,x}^T\, \mathrm{d}x\Delta v \\ & + \delta w^T \int_0^1 EA\, \varnothing_{w,x}\, w^2{}_{,x}\, \varnothing_{w,x}^T\, \mathrm{d}x\Delta w \\ & + \delta w^T \int_0^1 EA\, \varnothing_{w,x} w_{,x}\, v_{,x}\, \varnothing_{v,x}^T\, \mathrm{d}x\Delta v \\ & + \delta v^T \int_0^1 EA\, \varnothing_{v,x}\, v_{,x}\, w_{,x}\, \varnothing_{w,x}^T \mathrm{d}x\Delta w. \end{aligned} \tag{7}$$

Based on this project's purpose, only the formulas corresponding to calculating the displacement of the fabricated elements have been presented above. While the USFOS operates employing the green strain formulation concept, a more detailed explanation has been provided in [22]. To perform a nonlinear analysis with high technical accuracy, only an element located between each joint is required. Airy extrapolated, airy stretched, Stoke's 5th order, and stream function theory are carried out by USFOS. Other load cases could be easily combined with the proposed wave theories. Other principle waves considering uncertain sea environmental conditions could be modeled. Accordingly, USFOS is capable of adopting the worst sea state causing the most significant base shear or overturning moment. In performing a pushover analysis, the hydrodynamic forces caused by the critical wave phase are used. The buoyancy forces could be calculated independently from other existing hydrodynamic forces.

2. Developed Methodology

Employing deterministic approaches would not lead to achieving reliable results in OJPs' dynamic response since extreme wave loading has inherent uncertainty. Accordingly, in the present study, a methodology is developed to assess the OJPs' performance in a harsh ocean environment considering the stochastic behavior in wave loading. The outcome of the proposed approach is able to assist designers in predicting the OJPs' lifespan and improving their safety under harsh environmental conditions. This methodology consists of two main steps, as presented in Figure 1 and discussed in the following sections.

2.1. Structural Modeling. Simulating a complete structure model in software is necessary to measure the OJP response

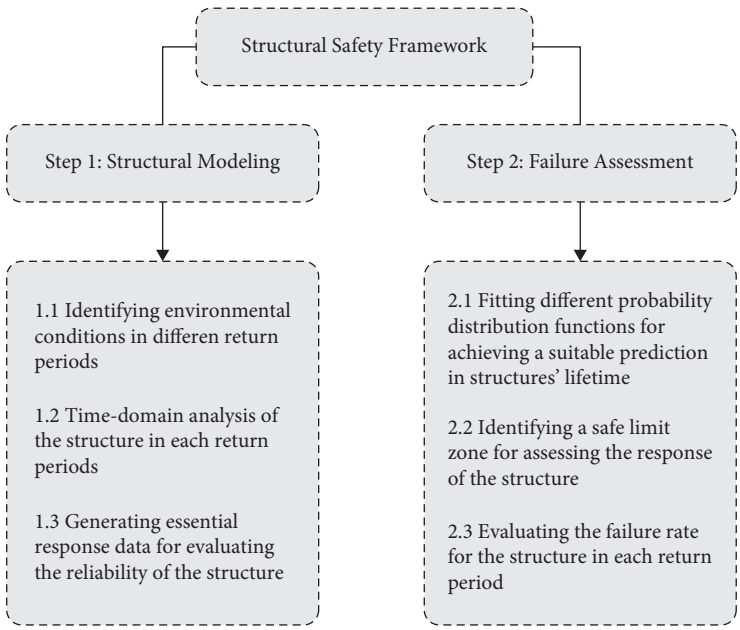

Figure 1: Developed methodology for assessing OJPs performance in a harsh environment.

more realistically. However, a multidegree of freedom (MDOF) system is suggested to be established by previous researchers [24–26]. Although using the MDOF model would significantly reduce the computational cost compared to a detailed model, it is a time-consuming procedure. It cannot also accurately evaluate structural components' response. The motion of an offshore structure subjected to wave loading can be found by solving an equation on the form:

$$m\ddot{x}(t) + c(x, \dot{x})\dot{x}(t) + k(x, \dot{x})x(t) = F(t), \quad (8)$$

where m is the mass of the system, $c(x, \dot{x})$ and $k(x, \dot{x})$ are the damping and the stiffness coefficients associated with the motion degree of freedom, respectively. $F(t)$ is the wave load acting on the mass in the direction of the selected degree of freedom.

Therefore, in the present study, USFOS software is adopted to overcome these concerns and simulate the whole structure as a detailed model to briskly obtain a more accurate response. The schematic of the OJP simulated in USFOS is illustrated in Figure 2.

Ocean waves have a random nature, which causes nonlinear forces on the OJPs. Therefore, a time-domain analysis will become necessary to obtain more accurate structural response results during extreme loading conditions. Accordingly, wave loads with different return periods corresponding to a certain significant wave height (H_s) and period (T) have been stochastically subjected to the structures. Consequently, the dynamic performance of the structures will be addressed in the principal return periods. Besides, a crucial factor in evaluating the performance of OJPs is the MBS forces that should be carried out to perform the global analysis of structures. Since the wave propagation across the members is different, all the locations will not be attaining the maximum forces in the structure. The MBS method may govern some jacket leg members near the seabed due to high shear. Similar to evaluating the performance of OJPs, due to the stochastic behavior of wave loadings, the MBS is carried out randomly. An 1800 second simulation has been performed to obtain the stochastic results in

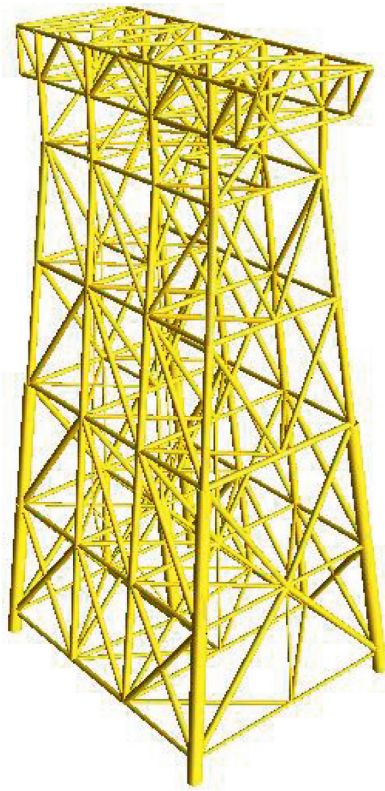

Figure 2: A schematic view of the OJP simulated in USFOS.

each return period for uncertain factors, including maximum deck displacement (MDD) and the base shear forces. The randomly obtained results in this step will be adopted to undertake a failure assessment.

2.2. Failure Assessment. Predicting the performance of OJPs due to the irregular nature of random ocean waves corresponding to stochastic wave height and period in each return period is associated with considerable uncertainties. Therefore, by considering the simulated data obtained from the previous step, structural modeling, the variables' uncertainty is modeled. A proper PDF is assigned to the uncertain parameters to perform the failure modeling of the OJP using MATLAB software. The maximum likelihood estimation (MLE) method is employed to estimate the MDD distribution properties by fitting suitable PDFs. The most appropriate PDF should be adopted to make a more reliable prediction of the OJP performance. To this end, following the suggested PDFs in [6, 27], some PDFs, including normal distribution, Weibull distribution, lognormal distribution, and generalized extreme value (GEV) distribution, are fitted on the obtained simulation data to choose the most appropriate PDF. On the one hand, a considerable number of numerical simulations are required to obtain a reliable distribution curve in the stochastic approach to predict the structure performance. On the other hand, if a known PDF can estimate the data obtained from a simulation procedure, the required number of simulations will be decreased significantly. It should be noted that this reduction is applicable since an offshore structure with the same structural properties has been previously considered in the same extreme wave conditions.

As mentioned earlier, the main reason for establishing nonlinear analysis of the OJP considering the drag forces and the structural stiffness for different DOF is examining their performance in a harsh environmental condition. In some return periods, due to the harsh environmental conditions and extreme wave loadings, the structure will exceed its survival limit, causing severe serviceability damages. Accordingly, a survival analysis corresponds to statistical approaches to investigate the time which an event of interest takes to occur should be carried out. The analysis will clarify that while the OJP is subjected to extreme wave loading, the performance will be in a safe condition or exceed its survival limit conditions. In this particular case, the survival analysis is carried out to investigate the lifetime of OJP. To this end, MATLAB software as a robust statistics and machine learning tool has been adopted. At first, a safe limit condition should be selected to observe those MDDs obtained from the simulation in USFOS that exceeds this limit. Consequently, the number of exceeded MDDs could be counted in the whole simulation time. During a survival analysis in this study, either an MDD is observed to fail at time T or the observation on that individual ceases at time c; the observation is then min (T, c); and an indicator variable I_c shows if the individual is censored or not. The calculations for hazard and survivor functions must be adjusted to account for censoring. Statistics and machine learning toolbox functions such as ecdf, ksdensity, coxphfit, and MLE account for censoring.

If the failure rate decreases with time, then the product exhibits infant mortality or early life failures. These types of failures are typically caused by mechanisms such as design errors, poor quality control, or material defects. The product exhibits a random or memoryless failure rate behavior if the failure rate is constant with time. Some possible causes of such failures are higher than anticipated stresses, misapplication, or operator error. If the failure rate increases with time, then the product wears out. These failures are caused by mechanisms that degrade the component's strength over time, such as mechanical wear or fatigue.

The survivor function is the probability of survival as a function of time. It is also known as the survival function. It gives the probability that the survival time of observed data exceeds a particular value. Since the cumulative distribution function, $F(t)$, is the probability that the survival time is less than or equal to a given point in time, the survival function for a continuous distribution, $S(t)$, is the complement of the cumulative distribution function:

$$S(t) = 1 - F(t). \tag{9}$$

The survivor function is also related to the hazard function. If the data have the hazard function, $h(t)$, then the survivor function is defined as follows:

$$S(t) = \exp\left(- \int_0^t h(u)\mathrm{d}u \right), \tag{10}$$

which corresponds to

$$S(t) = \exp\left(-H(t)\right), \tag{11}$$

where $H(t)$ is the cumulative hazard function.

The hazard function gives the instantaneous failure rate of an individual conditioned that the individual survived until a given time presented in the following equation:

$$h(t) = \lim_{\Delta t \longrightarrow \infty} \frac{P(t \le T < t + \Delta t | T \ge t)}{\Delta t}, \tag{12}$$

where Δt is a minimal time interval; therefore, the hazard rate is sometimes called the conditional failure rate. The hazard function always takes a positive value. However, these values do not correspond to probabilities and might be greater than 1.

The hazard function is related to the probability density function, $f(t)$, cumulative distribution function, $F(t)$, and survivor function, $S(t)$, as follows:

$$h(t) = \frac{f(t)}{S(t)} = \frac{f(t)}{1 - F(t)}, \tag{13}$$

which is also equivalent to

$$h(t) = -\frac{d}{dt} \ln S(t). \tag{14}$$

3. Application of the Developed Methodology: A Case Study

3.1. Scenario Development. An OJP as a real case study is considered in the North Sea encountered harsh environmental conditions to demonstrate the application of the proposed methodology. Some conventional studies have been conducted to investigate the OJPs' performance in the North Sea; however, the structures have not been exposed to harsh environmental conditions [28, 29]. In the present paper, an OJP encountered a harsh environmental condition in different return periods due to extreme wave loading for evaluating the structure's nonlinear dynamic behavior in survival conditions. Previous studies indicate several catastrophic failures on these structures operating in the North Sea due to harsh environmental conditions [30, 31]. Accordingly, there is still a need to develop a robust methodology to assess the structure's dynamic performance more realistically in harsh environmental conditions.

3.2. Structural Modeling. The dynamic performance of the OJP fabricated in the North Sea is assessed through a harsh environmental condition by employing USFOS for the structural simulation. Figure 2 shows the schematic of an 8-leg jacket implemented in a water depth of approximately 110 meters. The OJP legs are ordered in a two-by-four rectangular frame, while two central legs located on the north side of the platform are performing duties are launch runners. The top elevation of the structure is $27 * 54$ m, while there is a 20 m distance between the launch legs. The total structural height is 142 m, and the overall dimension considering the mud line is $56 * 70$ m. To transfer the horizontal forces, 5 bracings have been constructed on the structure. A rectangular module support frame (MSF) covering trusswork beams, 2 longitudinal, and 4 transverse trusses have been established. The trusswork is constructed at the height of 9.75 m and overall dimensions of $27 * 68$ m, as depicted in Figure 3.

Since the OJP foundation is a rectangular grid, it consists of 4 corners with 8 skirt piles widely used in offshore structure construction. X-braces are used from central to the corner legs at the bottom bay to improve the jacket frame's strength, while K-braces are used to strengthen the transverse frames. The stability of the conductor area is improved by establishing X-bracing. The OJP legs' diameter varies from 1.6 m to 3.0 m from the deck level to the elevation at $(-104)m$, respectively. Accordingly, vertical and horizontal braces vary in the intervals of $(1.1 - 1.6)m$ and $(0.8 - 1.0)m$, respectively. Regarding different elevations in the OJP, the ratio of tube diameter (D) to tube thickness (t) is not the same. The (D/t) properties for central legs, vertical braces, and horizontal braces in different elevations are summarized in Table 1.

The representative environmental conditions are applied to the simulated OJP in the North Sea for four different return periods suggested by Husain [1]. The wave loading on the structure is calculated according to the recommended procedure in the API-RP2A (API, 1994) by using the environmental parameters required to assess a fixed platform [32]. The wave loadings are calculated through Stoke's 5^{th} order nonlinear wave theory. The significant wave height during a storm condition could be modeled employing Rayleigh probability distribution [33, 34]. However, this study aims at conducting an extreme value analysis to assess the response of the OJP in the irregular state of the North Sea. Accordingly, the structure's response distribution would not necessarily follow a Rayleigh distribution in every return period. The simulation time for all four return periods is 1800 seconds in USFOS. The properties of extreme wave loadings acting on the simulated OJP are provided in Table 2.

According to the extreme nature of waves in the North Sea, a time-domain analysis in USFOS based on the Morison equation is performed. The Morison equation is a highly appreciated approach in hydrodynamics to solving wave forces in the time domain analysis [35]. The Morison equation consists of three main terms: the pressure field generated by the undisturbed waves, the inertia of the surrounding fluid, and the viscous drag [36]. The OJP is subjected to the suggested waves, including specific wave height in different return periods for 1800 seconds on the OJP stochastically. During the 1800 second simulation, more than 7200 discrete displacements are obtained, resulting in a more reliable and accurate OJP performance prediction. As shown in Figure 4, the platform's random displacement size increases dramatically from 1-year return period to 100-year return period. The MDD in the 1-year return period is approximately at $0.08m$, while it rises to roughly $0.2m$ in 100-year return period. Moreover, the MBS considering stochastic MDD is also determined for the global analysis of the OJP. As the wave propagates across the structure, the wave force on each member is different, and all the locations will not be attaining the maximum forces. Similar to the obtained random MDD, the MBS forces experience growth from the 1-year return period to 100-year return period. Stochastic base shear forces versus the MDD plotted in Figure 5 provide a precise overview of the OJP performance. It should be mentioned that the stochastic simulation of MDD would result in evaluating the performance of OJP probabilistically. Consequently, the OJPs' lifetime prediction will be addressed more reliable.

3.3. Failure Assessment. In the probabilistic approach, a great deal of numerical simulations is required to obtain a reliable analysis. Accordingly, more than 7200 discrete MDDs in 1800 seconds is achieved from the simulation in USFOS from the

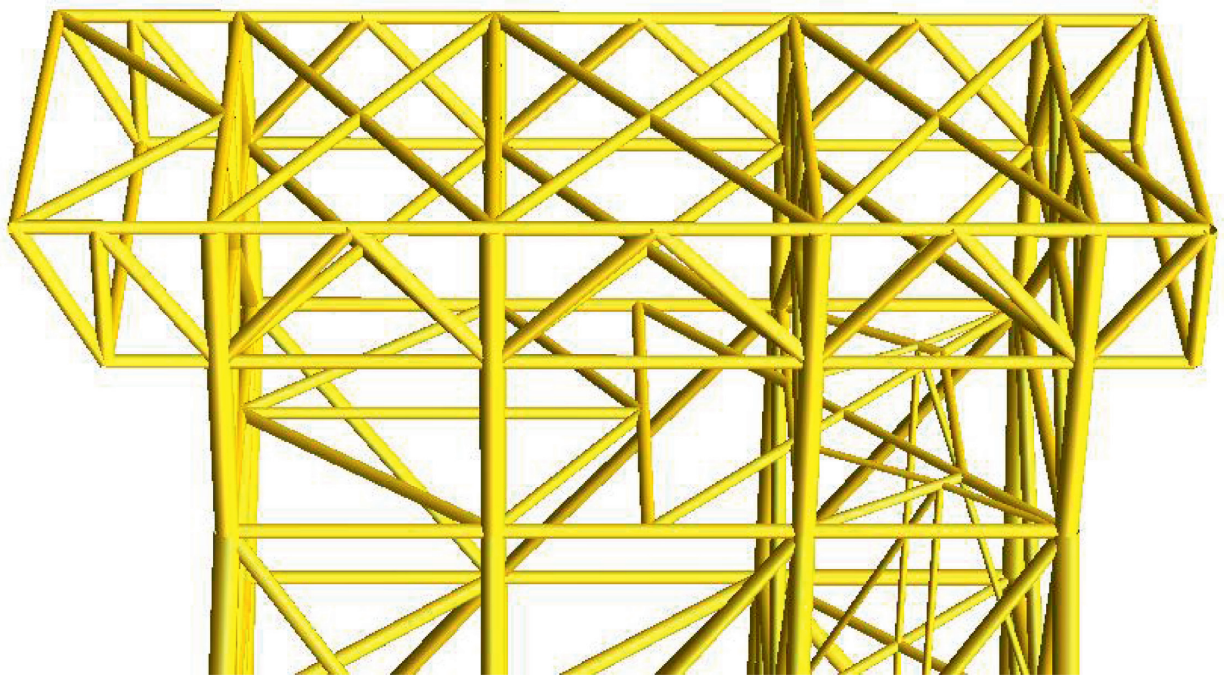

Figure 3: Module support frame simulated in USFOS.

Table 1: The ratio of tube diameter (D) to tube thickness (t) properties for central legs, vertical braces, and horizontal braces.

Element no.	(D/t)	Elevation (m)
1 (central leg)	(21 – 29)	(−14) to (−43)
2 (central legs)	(50 – 67)	(−43) to (−74)
3 (central legs)	80	(−74) to (−104)
4 (vertical braces)	43	(20 – 36)
5 (horizontal braces)	52	26 – 48
6 (horizontal braces)	20 – 33	(−14)

Table 2: Properties of extreme wave height during a 3-hour interval in the North Sea.

Return period (year)	Wave height (m)	Simulation time (sec)
1	19.11	1800
10	22.21	
50	24.08	
100	24.85	

previous step. In any histogram plot, the class (bins) width is considered to be equal for facilitating the interpretation. Particular attention should be devoted to the number of classes. Regarding too few classes would lead to the omission of some essential features of the data. Meanwhile, too many classes would result in an unclear overall picture due to high fluctuations in the frequencies [37]. Regarding researchers' recommendation in adopting suitable PDFs in literature [6, 27], four well-known PDFs, including normal, Weibull, lognormal, and generalized extreme value (GEV) distributions, are utilized to address the probabilistic characteristics of the MDDs in each return period. The role of PDFs is to estimate the behavior of the set of data. The selected PDFs should not precisely fit the obtained data since it would result in an overfitting concept [38, 39]. The assigned PDFs' unknown distribution parameters are also summarized in Table 3, employing the nonlinear least-squares method. The most significant advantage of nonlinear least-squares regression over many other techniques is the broad range of functions that can be fit. Although many scientific and engineering processes can be described well using linear models or other relatively simple models, there are many other processes which are inherently nonlinear processes [40]. Figure 6 contains 8 plots illustrated in two columns. On the one hand, the first column (on the left) consists of 4 plots that show the histogram of 7200 discrete MDDs obtained from 1800 second simulation in USFOS for different return periods. On the other hand, 4 other plots, illustrated on the second column (on the right), show the quantile-quantile plots (q-q plots). The q-q plots are employed as a graphical technique to examine whether two datasets come from populations with a typical distribution. The q-q plots in Figure 6 are developed considering three main components, including MDDs obtained from a simulation in USFOS (on the x axis), predicted MDDs (on the y axis), and the reference line ($y = x$).

The datasets should lie either up or down from the 45-degree reference line, while two datasets are distributed with a similar PDF. A significant advantage of a q-q plot is that several PDFs can be simultaneously tested. The q-q plot can provide more insights into the different nature of the data sets than analytical methods such as the chi-square and Kolmogorov–Smirnov. In this study, in Figure 6, the MDD obtained from stochastic modeling of USFOS is depicted versus the predicted MDD. The q-q plot technique is established to investigate the accuracy of assigned PDFs, including normal, Weibull, lognormal, and GEV distributions on MDD. As can be seen, the GEV distribution is appropriate for estimating the MDD results, while the lognormal distribution is not reliable in

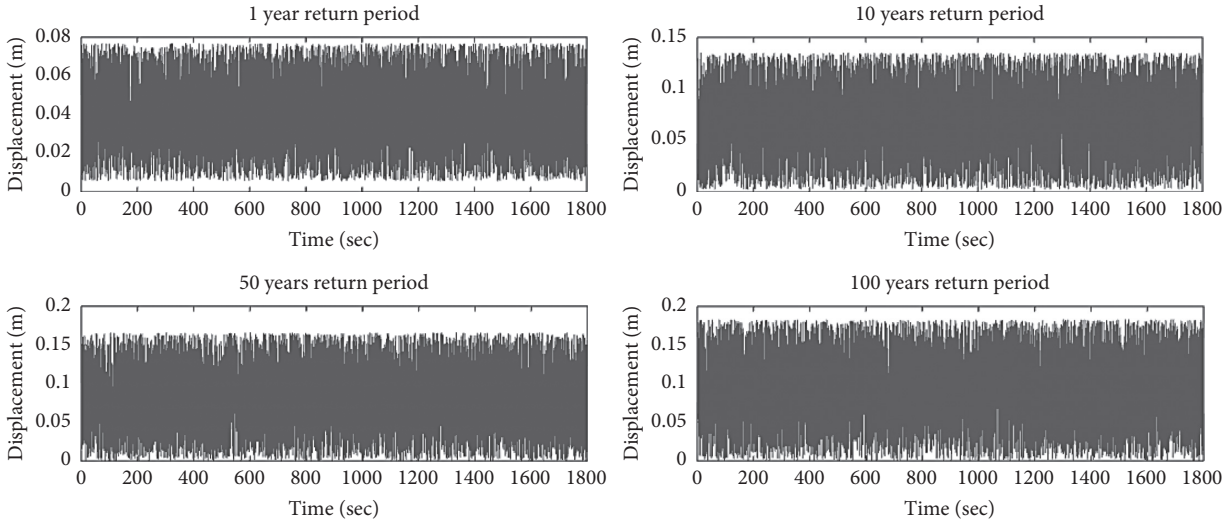

Figure 4: Stochastic displacement of offshore structure in 1800 seconds for four different return periods.

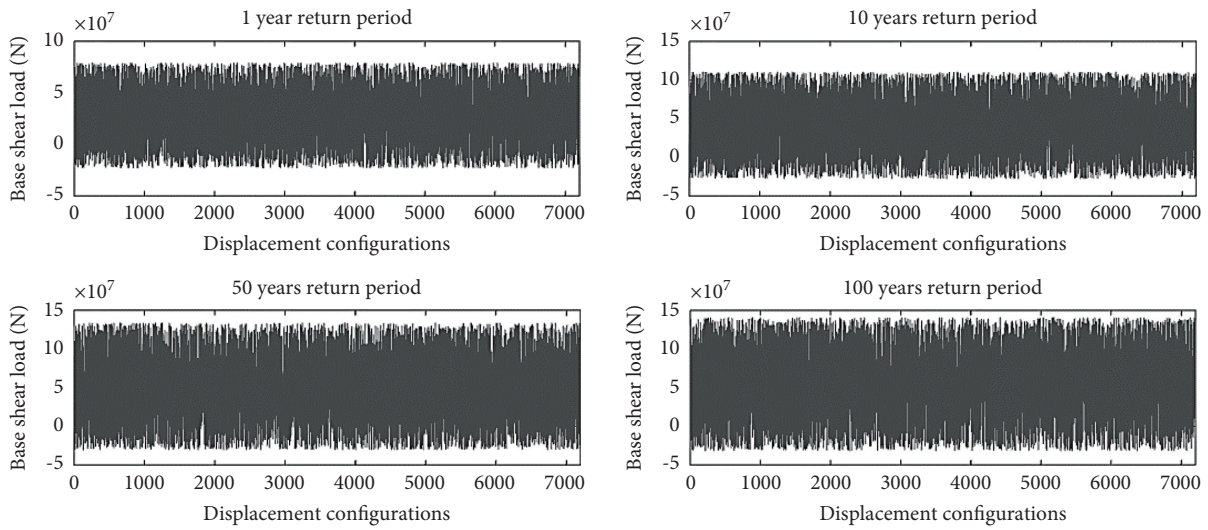

Figure 5: Stochastic pushover curves for four different return periods.

Table 3: Results of the fitted distributions on the maximum deck displacement obtained from maximum likelihood estimation (MLE).

Return period (year)	Distribution	Parameters
1	Normal	$\mu = 0.0410781$, $\sigma = 0.0206759$
	Weibull	$A = 0.0463619$, $B = 2.09065$
	Lognormal	$\mu = -3.36585$, $\sigma = 0.650225$
	Generalized extreme value (GEV)	$k = -0.429178$, $\mu = 0.0352711$, $\sigma = 0.0216415$
10	Normal	$\mu = 0.0687471$, $\sigma = 0.0386497$
	Weibull	$A = 0.0767069$, $B = 1.75138$
	Lognormal	$\mu = -2.93119$, $\sigma = 0.838403$
	Generalized extreme value (GEV)	$k = -0.439074$, $\mu = 0.0580849$, $\sigma = 0.040634$
50	Normal	$\mu = 0.0812511$, $\sigma = 0.0478613$
	Weibull	$A = 0.0896033$, $B = 1.59006$
	Lognormal	$\mu = -2.82105$, $\sigma = 0.993804$
	Generalized extreme value (GEV)	$k = -0.390447$, $\mu = 0.0668818$, $\sigma = 0.0491445$
100	Normal	$\mu = 0.0922143$, $\sigma = 0.0528807$
	Weibull	$A = 0.102039$, $B = 1.65111$
	Lognormal	$\mu = -2.67656$, $\sigma = 0.964783$
	Generalized extreme value (GEV)	$k = -0.443559$, $\mu = 0.0777447$, $\sigma = 0.0557262$

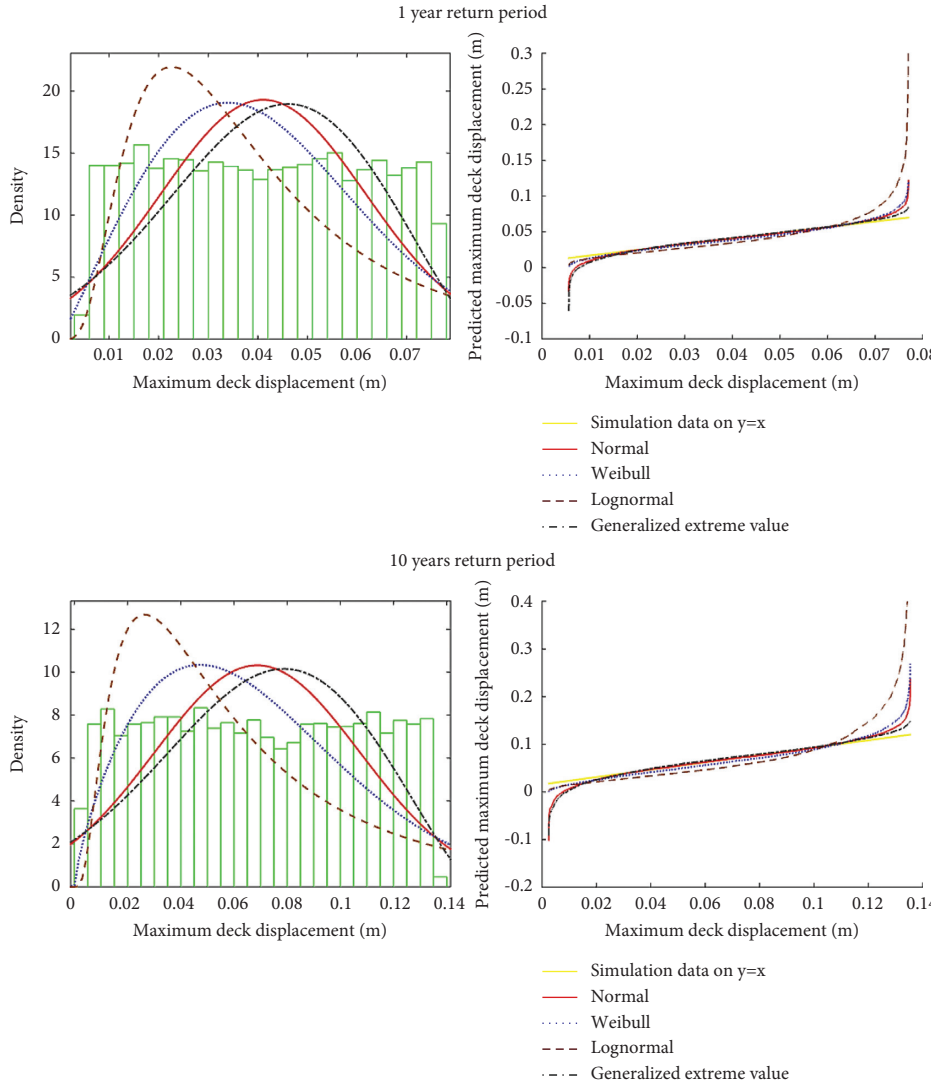

(a)

Figure 6: Continued.

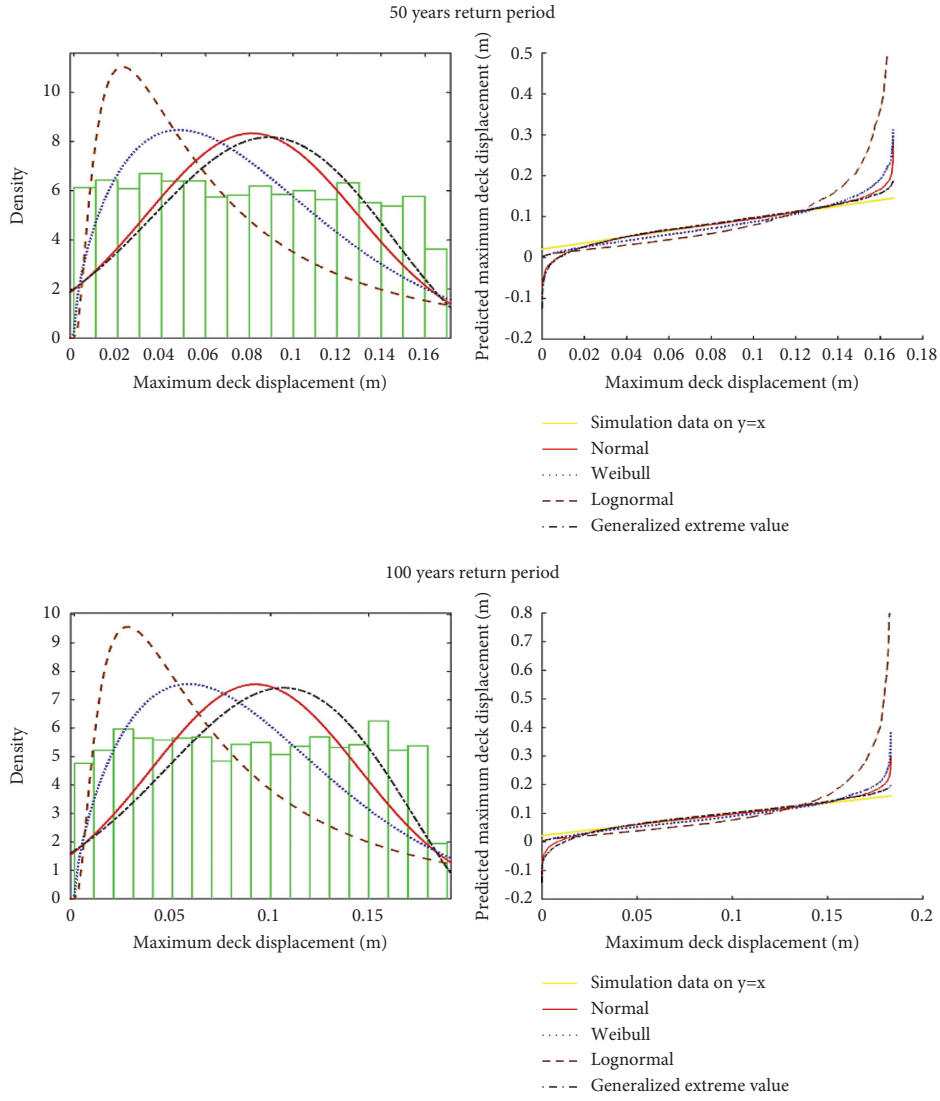

(b)

Figure 6: Different distributions fitted on the maximum deck displacement data resulted from USFOS software.

predicting the MDD in the return periods. Regarding Figure 6 and the q-q plot technique, GEV is the closest distribution to the reference line that shows the degree of appropriateness of the assigned distribution. Consequently, it is the reason for choosing the GEV as the most suitable distribution. Meanwhile, making a long-term prediction and explicit modeling of extreme values has been the main concern for researchers and engineers [41]. Accordingly, scientists have widely suggested GEV distribution to model extreme values due to its capability in extreme value modeling [42–45].

The cumulative distribution function (CDF) is utilized to determine whether the probability of a random observation is less, equal, or greater than a particular value. The CDFs of the MDDs for different return periods are illustrated in Figure 7. In 1-year return period, more than 50 percent of the MDDs are less than 0.04 meter while in 100-year return period are less than 0.1 meter. Accordingly, the more increment in MDDs would result in a growth in failure occurrence in the OJP lifetime. Furthermore, in 10 and 50-year return period, more than 50 percent of the MDDs are less than 0.072 and 0.082 meters, respectively.

The design and performance of the OJPs should satisfy the clients' and industry needs. Meanwhile, OJPs should continue their serviceability, considering the likely experienced displacement due to the harsh environmental condition. Accordingly, to predict the future performance of the OJPs, a fixed value as the safe limit condition should be assumed to conduct failure analysis. Consequently, a safe limit condition should be devoted to the OJP in every assumed return period. Regarding the previous studies [6, 30], the limit states should be adopted based on two main criteria: the crews' convenience on the

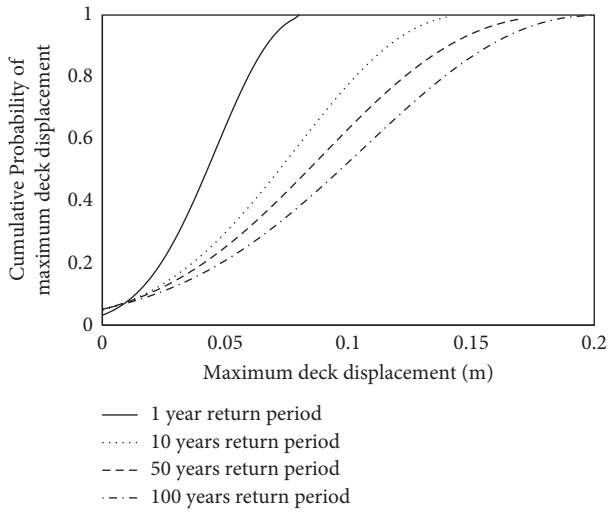

Figure 7: CDF of maximum deck displacement in 4 different return periods.

deck and maximum allowable deflection of the top node in the structure. Moreover, the assigned safe limit condition is firmly a function of the failure consequence purpose desired for design or operation. Meanwhile, other types of limit states, including ultimate loads and fatigue, are able to be incorporated with the proposed framework in this study to predict relevant failure probabilities. While the OJPs do not exceed the safe limit condition, the serviceability would continue with minor risk. Otherwise, the OJPs should be redesigned to satisfy the project requirements. Regarding earlier estimations, the dynamic performance of the fabricated OJP was evaluated in a harsh environmental condition considering four principal return periods. According to the results depicted in the figures, the most critical performance of the OJP is assessed considering the 100-year return period regarding the severe wave loadings. During a severe eave loading, the OJP may experience a transition and rotation, which results in an exceedance of the safe limit condition. To predict this event, the trajectory plot is developed considering the stochastic dynamic behavior of the OJP in the return periods. The trajectory plot would be illustrated by considering the OJP motion in the X and Y directions. Accordingly, a safe limit of 10 centimeters is considered for the OJP to explore the dynamic behavior in more detail. Figure 8 represents the trajectory motions of the OJP in the suggested return periods. As illustrated in Figure 8, during the storm condition in the simulation time of 1800 seconds, in a 1-year return period, the OJP would not pass the safe limit condition. In the other return periods, the number of exceedance in safe limit conditions increases significantly. The survival conditions are shown in the plots to clarify that OJP exceeds the critical limits. These graphs will play a vital role in the future failure analysis of the OJP as it shows the number of occurrences that the structure exceeds the safe limit condition. Regarding the severe wave loadings on the OJP, the structure strength and resilience will decrease, and the serviceability would suspend. These responses should be considered to improve the operation's safety and OJP performance's safety in different return periods [30].

Considering a safe limit condition at 10 centimeters as the fixed value for every return period, the OJP will continue its serviceability in a 1-year return period without a serious problem. Correspondingly, in the other three return periods, the OJP may experience some inevitable problems in performance. In this study, survival analysis is carried out to identify the time events in which the OJP exceeds the safe limit condition during the simulation time in 1800 seconds. The failure rate corresponding to the OJP performance is illustrated in Figure 9 for three different return periods. Due to the space limitations, the first 180 second results' derived from survival analysis are presented for the return periods to show the failure rate variation. A failure rate is simply a calculation of OJP exceedance from the safe limits, resulting in failures over time. It is usually first a frequency observation of how often the OJP has failed over some return periods. A failure rate can also predict the number of failures to be expected in given future periods. The failure rate is generally divided into rates of failure for each failure mechanism.

Regarding Figure 9, how the OJP exceeds the considered safe limit condition can be easily categorized due to the failure rate variation over time. When the failure rate tends to vary only with a change in wave loadings, the underlying mechanism is usually random. It should exhibit a constant failure rate as long as the environment stays constant. While the failure rate tends to increase with time and is logically linked with an aging effect, the underlying mechanism is time dependent. There is undoubtedly an aspect of randomness in the mechanisms labeled time dependent and the possibility of time

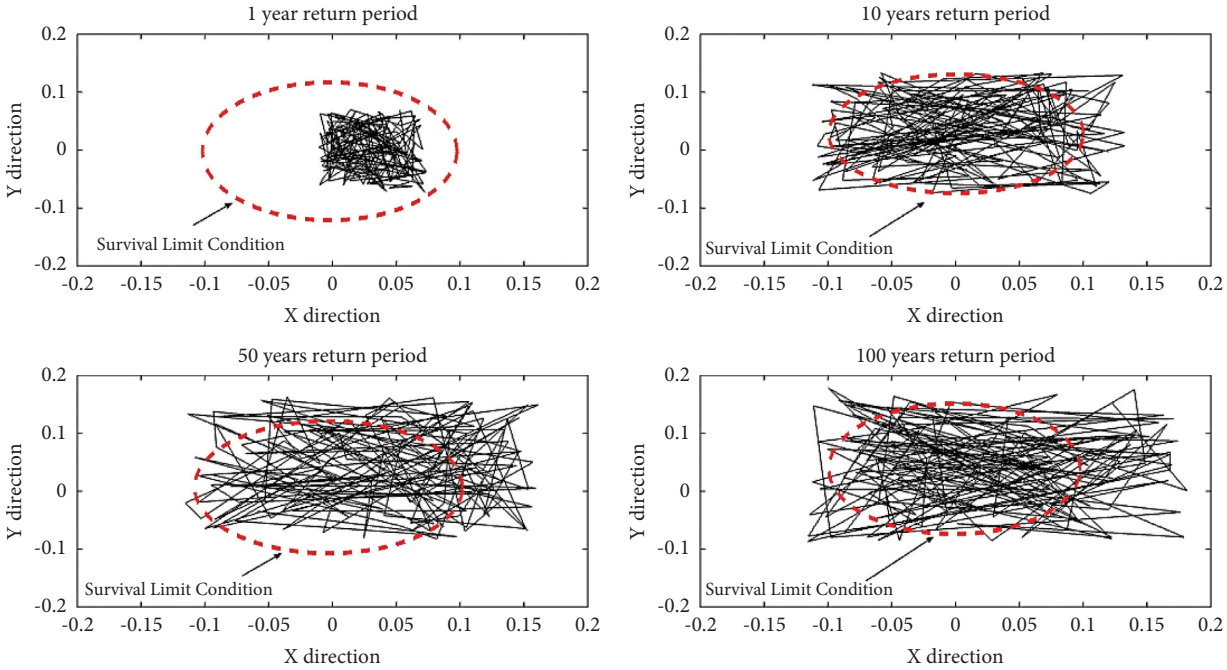

Figure 8: Trajectories of the OJP motions during the harsh environmental condition in four different return periods.

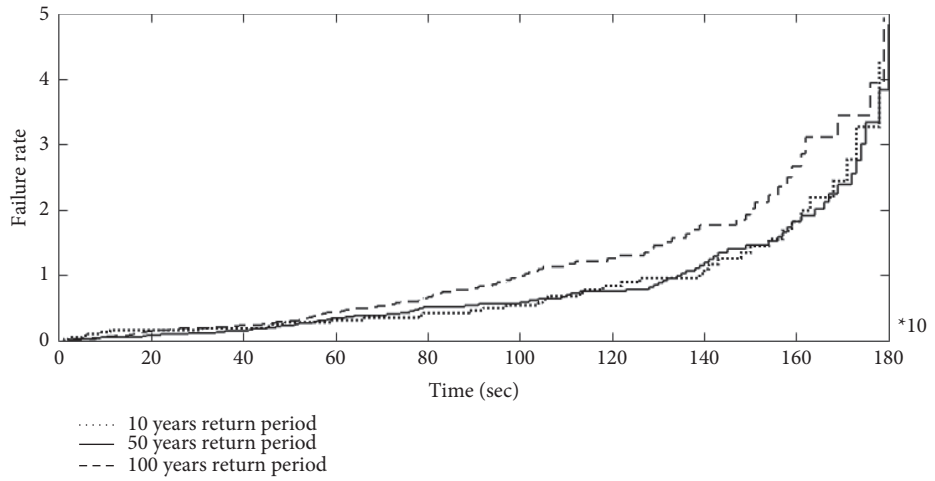

Figure 9: The failure rate corresponding to the OJP performance for three different return periods.

dependency for some of the mechanisms labeled random. The labels point to the probability estimation protocol that seems to be most appropriate for the mechanism.

4. Conclusions

This paper aims to develop a step-by-step methodology to assess the fabricated OJPs' reliability and failure rates during a harsh environmental condition at 4 principle return periods. The proposed methodology consists of two main steps. In the beginning, the structure of the fabricated OJP was simulated through the USFOS. Then, considering the ocean's random nature, various extreme wave loadings in different return periods were subjected to the OJP. Accordingly, probabilistic analysis has been carried out to evaluate the performance of the OJP. This methodology is able to evaluate the nonlinear dynamic response of the OJP during a storm and significantly reduce the time and computation cost of simulations. The application of the proposed framework was demonstrated by simulating an OJP in the North Sea during harsh environmental conditions. The dynamic analysis of the OJP shows that from 1-year to 100-year return periods, the MDD and MBS values will increase dramatically. Moreover, among all assigned PDFs on the stochastic MDD obtained from the simulation, the GEV distribution was the most appropriate for estimating the MDD results. The analysis results indicate that the OJP will not exceed the considered safe limit condition in 1-year return periods; however, it is likely to experience inevitable damages in other principal return periods. Also,

the OJP global trajectory for transition and rotational response demonstrates the effect of the different environmental conditions as well as stochastic waves on the performance of the OJP. Also, the failure rate of OJPs was evaluated regarding a safe limit condition (10 centimeters) in the principal return periods to carry out a more precise study. Regarding the highlighted and practical results of the proposed framework, potential future risks of the dynamic behavior of an OJP could be minimized. Designers and operators can adopt this robust framework to assess the reliability of the OJP encountering extreme sea wave loadings.

Data Availability

The data used to support the findings of this study are included within the article.

Conflicts of Interest

The authors declare that they have no conflicts of interest.

References

[1] M. K. A. Husain, *Determination of the 100-year Waveheight for the Forties Field in the North Sea*, Doctoral dissertation, University of Liverpool, Liverpool, UK, 2006.

[2] N. Harish, M. Sukomal, B. Shanthala, and R. Subba, "Analysis of offshore jacket platform," in *Proceedings of the Natl. Conf. On Sustainable Water Resources Management*, Surathkal; India, January 2010.

[3] G. Sandhya, "Analysis of offshore jacket platform," *International Research Journal of Engineering and Technology (IRJET)*, vol. 5, no. 1, 2018.

[4] S. M. Enderami, M. Zeinoddini, N. Shabakhty, and H. Ameryoun, "Dynamic non-linear analysis of offshore jacket type platforms under extreme wave loads," in *Proceedings of the International Conference on Offshore Mechanics and Arctic Engineering*, vol. 49095, pp. 593–601, Two Park Avenue NY, USA, January 2010.

[5] A. P. I. Rp2A-Wsd, *American Petroleum institute Recommended Practice for Planning, Designing and Constructing Fixed Offshore Platforms—Working Stress Design*, American Petroleum Institute, Washington, USA, 2007.

[6] M. A. Dastan Diznab, S. Mohajernassab, M. S. Seif, M. R. Tabeshpour, and H. Mehdigholi, "Assessment of offshore structures under extreme wave conditions by Modified Endurance Wave Analysis," *Marine Structures*, vol. 39, pp. 50–69, 2014.

[7] K. A. Digre and F. Zwerneman, "Insights into using the 22nd edition of API RP 2A recommended practice for planning, designing and constructing fixed offshore platforms-working stress design," in *Proceedings of the Offshore Technology Conference*, Offshore Technology Conference, Houston, Texas, USA, April 2012.

[8] C. Iso, "Bases for Design of Structures-Assessment of Existing Structures," Report ISO 13822:2010, Slovak Office of Standards, Metrology and Testing, Bratislava, Slovak, 2012.

[9] A. BahooToroody, M. M. Abaei, F. BahooToroody, F. De Carlo, R. Abbassi, and S. Khalaj, "A condition monitoring based signal filtering approach for dynamic time dependent safety assessment of natural gas distribution process," *Process Safety and Environmental Protection*, vol. 123, pp. 335–343, 2019.

[10] S. Khalaj, F. BahooToroody, M. Mahdi Abaei, A. BahooToroody, F. De Carlo, and R. Abbassi, "A methodology for uncertainty analysis of landslides triggered by an earthquake," *Computers and Geotechnics*, vol. 117, Article ID 103262, 2020.

[11] F. BahooToroody, S. Khalaj, L. Leoni, F. De Carlo, G. Di Bona, and A. Forcina, "Reliability estimation of reinforced slopes to prioritize maintenance actions," *International Journal of Environmental Research and Public Health*, vol. 18, no. 2, p. 373, 2021.

[12] L. Leoni, A. Cantini, F. BahooToroody et al., "Reliability estimation under scarcity of data: a comparison of three approaches," *Mathematical Problems in Engineering*, vol. 2021, Article ID 5592325, 15 pages, 2021.

[13] L. Leoni, F. BahooToroody, S. Khalaj, F. D. Carlo, A. BahooToroody, and M. M. Abaei, "Bayesian estimation for reliability engineering: addressing the influence of prior choice," *International Journal of Environmental Research and Public Health*, vol. 18, no. 7, p. 3349, 2021.

[14] A. Fayazi and A. Aghakouchak, "Reliability Based Assessment of Existing Fixed Offshore Platforms Located in the Persian Gulf," *InternaionalJournal of Maritime Technology*, vol. 4, 2015.

[15] R. G. Bea and M. Mortazavi, "Experimental validation of the ULSLEA with results from frame tests," in *Proceedings of the 7th International Offshore and Polar Engineering Conference*, Honolulu, Hawaii, May 1992.

[16] L. Manuel, D. G. Schmucker, C. A. Cornell, and J. E. Carballo, "A reliability-based design format for jacket platforms under wave loads," *Marine Structures*, vol. 11, no. 10, pp. 413–428, 1998.

[17] G. Ersdal, "Assessment of Existing Offshore Structures for Life Extension," University of Stavanger, Stavanger, Norway, Department of Mechanical and Structural Engineering and Material Sciences, 2005.

[18] A. M. Cruz and E. Krausmann, "Damage to offshore oil and gas facilities following hurricanes Katrina and Rita: an overview," *Journal of Loss Prevention in the Process Industries*, vol. 21, no. 6, pp. 620–626, 2008.

[19] H. Kjeøy, N. G. Bøe, and T. Hysing, "Extreme-response analysis of jack-up platforms," *Marine Structures*, vol. 2, no. 3-5, pp. 305–334, 1989.

[20] A. C. Morandi, P. A. Frieze, M. Birkinshaw, D. Smith, and A. Dixon, "Jack-up and jacket platforms: a comparison of system strength and reliability," *Marine Structures*, vol. 12, no. 4-5, pp. 311–325, 1999.

[21] K. van Raaij and O. T. Gudmestad, "Wave-in-deck loading on fixed steel jacket decks," *Marine Structures*, vol. 20, no. 3, pp. 164–184, 2007.

[22] SINTEF Group, *USFOS Getting Started*, Structural Engineering, Marintek, 2001, https://www.usfos.com/manuals/usfos/theory/documents/Getting_Started.pdf..

[23] G. Mallik and N. Nataraj, "A nonconforming finite element approximation for the von Karman equations," *ESAIM: Mathematical Modelling and Numerical Analysis*, vol. 50, no. 2, pp. 433–454, 2016.

[24] N. S. Mastanzade and G. Yazici, "Dynamic Behavior and Optimization of Offshore Gravity Platforms," *Journal of Offshore Mechanics and Arctic Engineering*, vol. 127, 2005.

[25] D. H. Kim, "Neuro-control of fixed offshore structures under earthquake," *Engineering Structures*, vol. 31, no. 2, pp. 517–522, 2009.

[26] A. A. Golafshani and A. Gholizad, "Friction damper for vibration control in offshore steel jacket platforms," *Journal of Constructional Steel Research*, vol. 65, no. 1, pp. 180–187, 2009.
[27] H. Ahmadi and V. Mayeli, "Development of a probability distribution model for the LJF factors in offshore two-planar tubular DK-joints subjected to OPB moment loading," *Marine Structures*, vol. 63, pp. 196–214, 2019.
[28] M. Vilnay, V. Sivickij, F. Watters, C. Doerich-Stavridis, and L. Chernin, "Fidelity of computational modelling of offshore jacket platforms," *Proceedings of the Institution of Civil Engineers - Engineering and Computational Mechanics*, vol. 172, no. 2, pp. 79–93, 2019.
[29] X. Han, W. Qiao, and B. Zhou, "Frequency domain response of jacket platforms under random wave loads," *Journal of Marine Science and Engineering*, vol. 7, no. 10, p. 328, 2019.
[30] M. M. Abaei, E. Arzaghi, R. Abbassi, V. Garaniya, and S. Chai, "A novel approach to safety analysis of floating structures experiencing storm," *Ocean Engineering*, vol. 150, pp. 397–403, 2018.
[31] W. Brindley and A. P. Comley, "North sea mooring systems: how reliable are they?" in *Proceedings of the International Conference on Offshore Mechanics and Arctic Engineering*, vol. 45370, June 2014.
[32] S. Lacasse and P. Boisard, "Consequence of new API RP2A guideline for piles in soft clay," in *Proceedings of the International Conference on Soil Mechanics and Foundation Engineering*, pp. 527–530, New Delhi, India, 1994.
[33] F. J. Méndez, M. Menéndez, A. Luceño, R. Medina, and N. E. Graham, "Seasonality and duration in extreme value distributions of significant wave height," *Ocean Engineering*, vol. 35, no. 1, pp. 131–138, 2008.
[34] C. Vidal, R. Medina, and P. Lomónaco, "Wave height parameter for damage description of rubble-mound breakwaters," *Coastal Engineering*, vol. 53, no. 9, pp. 711–722, 2006.
[35] I. Fylling, K. Mo, K. Merz, and N. Luxcey, *Floating Wind Turbine-Response Analysis with Rigid-Body Model*, European Offshore Wind, Scotland, UK, 2009.
[36] W. Yang and Q. Li, "The expanded Morison equation considering inner and outer water hydrodynamic pressure of hollow piers," *Ocean Engineering*, vol. 69, pp. 79–87, 2013.
[37] H. Ahmadi and M. A. Lotfollahi-Yaghin, "A probability distribution model for stress concentration factors in multiplanar tubular DKT-joints of steel offshore structures," *Applied Ocean Research*, vol. 34, pp. 21–32, 2012.
[38] X. Ying, "An overview of overfitting and its solutions," *Journal of Physics: Conference Series*, vol. 1168, Article ID 022022, 2019.
[39] D. M. Hawkins, "The problem of overfitting," *Journal of Chemical Information and Computer Sciences*, vol. 44, no. 1, pp. 1–12, 2004.
[40] X. Yang and Z. You, "New predictive equations for dynamic modulus and phase angle using a nonlinear least-squares regression model," *Journal of Materials in Civil Engineering*, vol. 27, no. 3, Article ID 04014131, 2015.
[41] T. H. Soukissian and C. Tsalis, "The effect of the generalized extreme value distribution parameter estimation methods in extreme wind speed prediction," *Natural Hazards*, vol. 78, no. 3, pp. 1777–1809, 2015.
[42] I. A. Chaves and R. E. Melchers, "Extreme value analysis for assessing structural reliability of welded offshore steel structures," *Structural Safety*, vol. 50, pp. 9–15, 2014.
[43] N. V. Teena, V. Sanil Kumar, K. Sudheesh, and R. Sajeev, "Statistical analysis on extreme wave height," *Natural Hazards*, vol. 64, no. 1, pp. 223–236, 2012.
[44] A. Lu, L. Zhao, Z. Guo, and Y. Ge, "A comparative study of extreme value distribution and parameter estimation based on the Monte Carlo method," *Harbin Gongye Daxue Xuebao*, vol. 45, no. 2, pp. 88–95, 2013.
[45] R. Mínguez, M. Menéndez, F. J. Méndez, and I. J. Losada, "Sensitivity analysis of time-dependent generalized extreme value models for ocean climate variables," *Advances in Water Resources*, vol. 33, no. 8, pp. 833–845, 2010.